Multiobjective-Multipoint Rotor Blade Optimization in Forward Flight Conditions Using Surrogate-Assisted Memetic Algorithms

Andrea Massaro
Aerodynamic Specialist
AgustaWestland, Aerodynamics Dept.
andrea.massaro@agustawestland.com

Andrea D'Andrea*
Rotor Aerodynamics Technical Leader
AgustaWestland, Aerodynamics Dept.
andrea.dandrea@agustawestland.com

Ernesto Benini
Professor
University of Padova, Mechanical Dept.
ernesto.benini@unipd.it

ABSTRACT

A multi-objective and multi-point optimization framework for helicopter rotor performance is presented. This framework is based on a multi-objective surrogate-assisted memetic algorithm which is coupled with two aerodynamic solvers for rotor performance prediction: a lifting-line comprehensive tool and a more advanced three-dimensional panel method coupled with a constant vorticity contour free-wake vortex model. The purpose is to improve aerodynamic performance of helicopter main rotors in multi-point forward flight operations by searching for optimal blade shape. The optimization procedure and the memetic algorithm are first described. Afterwards, they are applied to optimization of several features of a blade, like twist, chord and sweep and the outcomes from those optimizations are discussed from an aerodynamic viewpoint. The advantages of the proposed optimization procedure are finally illustrated and compared to more traditional techniques.

INTRODUCTION

The aerodynamic optimization of the main rotor is one of the most important aspects on the entire design of an helicopter, since it affects the performance and the capabilities of the aircraft at all flight conditions and, being the main source of power requirement, can drastically change the characteristics of the helicopter, e.g. total range and top speed. The extreme variability of the conditions in which an helicopter operates, makes the optimization problem highly complex and multi-objective. The possibility of using multi-objective evolutionary algorithms on the field of blade rotor optimization has been precluded up to now due to the inefficiency of such kind of algorithms, that typically requires a large number of aerodynamic simulations. The development of high efficiency memetic algorithms (based on more common genetic algorithms) makes possible their application to rotor optimization.

It has been evidenced by several relatively recent surveys [1,2] which are the main issues encountered by the helicopter optimization community during the last two decades. These assessments are mainly focused on dynamic optimization of rotors, therefore on the structural viewpoint, but similar conclusions can be drawn for pure aerodynamic rotor optimizations. This is particularly true if we consider that quite often the same code is used to predict aerodynamic performance or structural/dynamic loads, e.g. aeromechanic comprehensive codes. Ref. [1] highlights the major problem of the accuracy of the numerical tools used to predict rotor performance, in fact optimization results obtained using analysis of insufficient accuracy have very limited worth. On the other hand, as the reliability of predicting tools increases, the most important features that drive the flow behavior over a rotor can be captured, making optimization a trusted way for rotor performance enhancement. Usually, accuracy improvement of rotor performance predictions leads to a substantial increase of computational demand [2], e.g. unsteady panel methods or computational fluid dynamics. The growing of computational capabilities and large scale parallel computers help to mitigate this problem and optimizations using such kind of codes are nowadays possible. Finally, the optimization algorithm is identified as a critical parameter [1,2]. This aspect has largely delayed the diffusion of optimization algorithm based design within the industrial area, because of the typical inefficiency of the available algorithms and the trouble process of integrating commercial codes with the algorithms themselves. However, several works have been carried out during the past years on rotor aerodynamic optimization, in which the traditional gradient-based optimization method is probably the mainstay algorithm. The well-known issue of such algorithms is the high sensitivity to local minima. To overcome the problem, nongradient-based stochastic algorithms have also been used, like genetic algorithms and simulated annealing. Response surface method [3] and hybrid approaches have been identified [2] as promising methods to enhance efficiency, reducing the number of aerodynamic simulations required and increasing the convergence rate.

Several examples of rotor aerodynamic optimizations have been found in open literature. A tool for aerodynamic optimization of rotors was firstly presented in [4], based on the comprehensive analysis program CAMRAD/JA [5] as flow solver and the gradient-based optimizer CONMIN [6]. The horse power minimization at hover and forward flight conditions, properly combined into a weighted sum, was chosen as objective and a tapered planform was optimized together with the twist distribution. Similar approach has been developed in [7,8] in which an integrated aerodynamic/dynamic optimization was carried out, introducing also blade structural properties as design variables. In [9] a circulation optimization along the blade span was proposed with the aim of minimizing the induced power loss on a rotor in hover and forward flight. A multi-level decomposition technique has been developed in [10] dealing with an integrated aerodynamic/dynamic optimization and based on gradient-based algorithm. By means of the multi-level decomposition method,

Presented at the 37th European Rotorcraft Forum, Gallarate, Italy, Sep. 13-15, 2011.
* Corresponding Author

aerodynamic and dynamic design was performed at a global level while the structural design was carried out at a detailed level. Response surface method (RSM) was used in [11] together with a gradient-based algorithm in order to reduce the total number of objective function evaluations, i.e. aerodynamic or dynamic simulations of the rotor. More recently, Reynolds-averaged Navier-Stokes (RANS) methods have been widely used in prediction of rotor performance, especially for hover condition. The advances in computational fluid dynamics (CFD) and the growing of computational capability have made possible the application of these methods to optimization. An example is found in [12] where the CONMIN optimizer is coupled with a CFD code for rotor optimization in hover. The trim information necessary to run a CFD simulation are computed using a simpler lifting-line solver. Twist, chord, sweep and anhedral have been considered separately for as many optimizations. Moreover, adjoint methods [13] coupled with CFD solvers received much attention during the last years, due to the fact that the computational expense incurred in the calculation of the complete gradient is effectively independent of the number of design variables. The application of the adjoint method for helicopters in hover can be found in [14,15], while the same optimization problem was addressed for tiltrotors in [16]. Examples of application of evolutionary algorithms for helicopter rotor optimization are also available in literature. In [17] a lifting-line solver was used to predict performance of a rotor in hover and forward flight conditions, together with a two-dimensional interactive boundary-layer code to optimize blade sections. The method was based on a single-objective genetic algorithm with the aim of minimizing horse power. A very recent work [18] was also published where RSM, based on a CFD database, was used in conjunction with a single-objective genetic algorithm to optimize several aspects of rotor blades in hover and forward flight separately.

In the present paper, the authors illustrate a framework for rotor blade aerodynamic optimizations, based on a state-of-the-art multi-objective surrogate-assisted memetic algorithm (SAMA). Such an algorithm extends the concept of RSM applied to genetic algorithms (GAs) with the advantages of robust global search based on GA and local search based on more efficient gradient-based algorithms. From an aerodynamic viewpoint, this multi-objective optimizer is coupled with two interconnecting codes, which are CAMRAD/JA [5] and the AgustaWestland in-house-developed code ADPANEL [19], a panel method tool coupled with a constant vorticity contour (CVC) free wake vortex model. Several applications to rotor blade optimization in forward flight conditions are presented and discussed. It is worth noting that the ultimate aim of the present work is not only to show optimal rotor blade shapes, but to develop and validate an efficient methodology for multi-objective optimization of rotors, with intention to couple this strategy, in the close future, to more complex and computational demanding aerodynamic tools, like for instance RANS solvers.

PROBLEM FORMULATION

The present work was aimed at optimizing the aerodynamic performance of a rotor in forward flight conditions searching for optimal planform shape of the blade. The main objective of the optimizations is minimization of horse power required by a generic helicopter main rotor in the aforementioned flight conditions. As previously stated, the optimization approach is based on a multi-objective and multi-point methodology that, from a designer point of view, leads to many advantages. As a matter of fact, this approach generates a Pareto optimal frontier composed of several equally optimal solutions. These overabundant information allow the designer to select the final geometry considering also different aspects than the pure aerodynamic performance.

In detail, the optimization problem under consideration is a two-objective minimization problem and each objective is related to a different flight. Table 1 summarizes the conditions used for the optimizations, that are two high-speed forward flights at different altitudes:

Condition	Altitude ASL [m]	Aircraft speed [kts]
C1	0	150
C2	5150	140

Table 1: Optimization flight conditions (ISA).

The objectives of the optimization problem under consideration are defined in Eq. 1 as follows:

$$\mathbf{F}(\mathbf{x}) = \begin{cases} F_1(\mathbf{x}) = Pw_{C1} \\ F_2(\mathbf{x}) = Pw_{C2} \end{cases}, \qquad (1)$$

where **x** is the vector describing the blade geometry, F_i are the components of the objective function **F** and *Pw* is the main rotor horse power to minimize. The hover performance are not taken into account in Eq. 1 since the main aim of the present work is blade shape optimization for fast forward flight. However, a post-check constraint is defined at hover conditions out of ground effect (HOGE), due to the high importance of this condition for an aircraft. The rotor figure of merit (*FM*) of the optimized blades must not be lower that the baseline value:

$$FM_{HOGE,opt} \geq FM_{HOGE,baseline}. \qquad (2)$$

A limited number of optimized blades are also selected and analyzed at different altitudes and velocities. Table 2 lists the three different altitudes considered during this post-processing analysis (ISA+0 conditions). Velocities vary from hover up to maximum achievable speed for a specified altitude.

Name	Altitude ASL [m]	Density ratio [ρ/ρ_0]
Flight1	0	1
Flight2	3260	0.723
Flight3	5150	0.591

Table 2: Post-processing flight conditions.

The baseline rotor configuration, used for comparison with the optimized solutions, is composed of five rectangular blades with a non-dimensional chord of 0.068 (with respect to the radius *R*). All the optimizations are carried out considering an isolated single main rotor without the fuselage, to avoid useless time loss. The radius *R* is set to 6.9m and the tip speed V_{tip} is 215m/s. No sweep and anhedral are present in the baseline blade and a linear spanwise twist is considered. The twist slope is -9.4º/*R* and the twist value at the tip is chosen to be equal to -1.5º. To calculate the thrust required by the rotor a 6500kg weight helicopter is chosen. The weight is kept constant for all the flight conditions.

BLADE GEOMETRY PARAMETERIZATION

The description of the blade geometry is based on four basic parameters, typically used to define a rotor blade: twist, chord, sweep and anhedral. These four parameters can be optimized separately or together during an optimization process, choosing any possible combination. When one parameter is not optimized, its distribution is kept constant during the optimization and equal to the baseline distribution, initially defined by the user. All the parameters are defined by means of b-spline curves [20]. This strategy permits to define smooth distributions with limited number of control points, allowing also the user to choose the curve's order (that controls the curve's smoothness). Moreover, the blade can be described by b-splines entirely or partially. The radial position of the control points is freely defined by the user (allowing local refinements, e.g. more dense concentration at the tip) and it is kept fixed during the optimization, while the remaining coordinate of the control points are the design variables for the optimizer.

The main aspects of the blade, that are twist, chord and sweep, have been parameterized using the aforementioned technique and the different characteristics of each parameter are shown in Table 3. While twist and chord are described for all the length of the blade (the b-spline curve starts at 0.09 r/R, that is slightly above the hub radius), sweep is defined starting from 0.4 r/R. Anhedral is not considered in the present work so it is not visible in Table 3.

Parameter	Start [r/R]	End [r/R]	N. control points
twist	0.09	1	7
chord	0.09	1	8
sweep	0.4	1	5

Table 3: Parameterization intervals and number of control points for each parameter.

As previously said, the optimization algorithm treats the b-spline's control points like generic design variables and these points are allowed to move inside a predefined range of variation. Each variable has its own range, that can be different from the range of another one. A range of variation is entirely defined by a lower and an upper bound and the user must specify these values for all the design variables. Figure 1 shows the bounds used for the present work, respectively for twist, chord and sweep.

PERFORMANCE ANALYSIS PROGRAMS

The present optimization tool makes use of different aerodynamic codes for rotor blade design. In particular, two aerodynamic solvers have been selected: a comprehensive code like CAMRAD/JA [5], based on lifting-line and momentum theories, and a more accurate and advanced three-dimensional panel method coupled with a state-of-the-art free-wake vortex model, that is ADPANEL [19]. The optimization algorithm can manage both the solvers in an automated way without intervention of the user. The former is provided with an internal trimmer, while the latter needs information of rotor trim from an external source. For this reason, when ADPANEL is used CAMRAD/JA is preventively run to compute the rotor trim and these data are given to the panel code. Unfortunately, the CAMRAD/JA trim is not always able to assure exact values of rotor thrust when performance are calculated again in

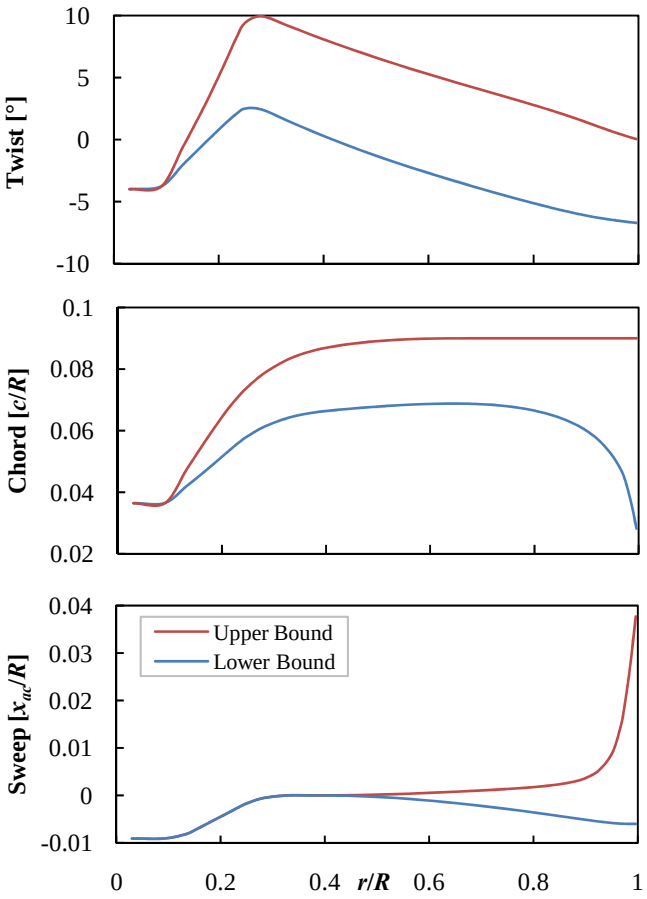

Figure 1: Range of variation for Twist, Chord and Sweep.

ADPANEL and this fact complicates further the optimization problem. To overcome this issue, two additional design variables are added to the optimization problem and the algorithm, during the optimization course of events, can change not only blade shape but also collective pitch of the whole rotor. In this manner, the algorithm chases optimal blades that assure minimum power with the required thrust. For both the solvers the assumption of rigid blade is used.

CAMRAD/JA code

The rotor aerodynamic model in CAMRAD/JA is based on lifting-line theory, using steady two-dimensional airfoil coefficient tables. Despite the possibility of introducing several complex features to increase the physical adherence of the model to reality, the philosophy used in the present work is the simplicity. The induced velocity on the main rotor is calculated from the momentum theory, without a time-marching wake model, and no additional unsteady effects (like dynamic stall) are introduced. It results in a quick and reliable analysis tool, with very high percentage of converged individuals. The robustness of the aerodynamic tool is a fundamental characteristic to preserve efficiency of the optimization algorithm.

ADPANEL code

ADPANEL is a full-unstructured panel method coupled with a time-stepping full-span free wake vortex model. Present tool implements the most advanced aerodynamic features in the field of potential methods, such as the capability to represent the geometrical surfaces into unstructured-hybrid meshes, a constant vorticity contour (CVC) modeling of both rotary and fixed wing wakes, and a

multi-processor implementation. Thanks to the previous features, ADPANEL is able to analyze in short computational times and with detailed predictions entire helicopter and tiltrotor configurations even operating in ground effect. The wake modeling implemented in ADPANEL is composed of two parts: a "dipole buffer wake sheet", and a set of "constant vorticity contour vortex filaments". Buffer wake and CVC vortex filaments are used to represents the vorticity released from rotary and fixed wings for both their components, trailed and shed. The CVC free-wake modeling developed in ADPANEL allows to generate refined roll-ups and high spanwise resolution along rotor blades without enforcing an unnecessary large number of wake elements. Figure 2 shows an example of the computed CVC wake development in case of a full-helicopter configuration operating OGE (AW101). Recent and validated "vortex dissipation laws" have been implemented in ADPANEL in order to represent the increasing of the vortex core with the time passing. Detailed information on both theory and validation of present tool can be found in [19,21-23].

OPTIMIZATION ALGORITHM

The optimization algorithm used in the present work belongs to the family of the surrogate-assisted memetic algorithms (SAMA). Memetic algorithms (MAs) are population-based metaheuristich search methods inspired by Darwinian principles of natural evolution and Dawkins notion of a "meme", defined as a unit of cultural evolution that is capable of local refinements [24,25]. The main advantage of MAs over concurrent strategies lies in creating a synergy between global and local search. The global searcher should be able to explore the entire design space, selecting the best solutions in terms of their objective values, while the local searcher should improve further the solutions by means of small local changes in a time-efficient way. A genetic algorithm (GA) is the most appropriate choice as global search algorithm since it is insensitive to local minimum and can easily handle multi-objective optimization problems (MOOPs). The local search is carried out using a gradient-based algorithm that tries to improve the objective function using a surrogate model (SM) of the function itself. This method allows a very efficient local improvement of the individuals coming from a GA population, as the SM can be evaluated much faster than the original aerodynamic analysis. The time spent to estimate the local improvements is far less than that required for a single ADPANEL simulation. The drawback of this method lies on the approximated nature of the SM, but this is overcome by the improved achievable convergence rate. The use of an approximated model leads to the so-called SAMA approach.

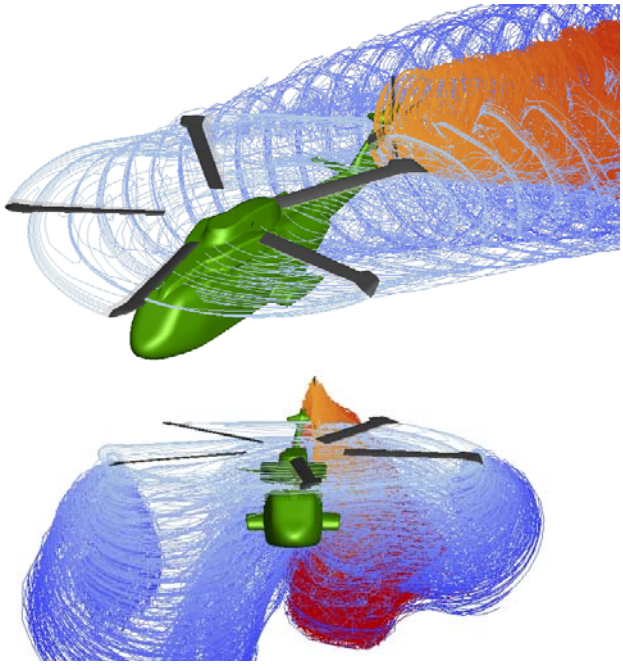

Figure 2: ADPANEL CVC wake development for a full-rotorcraft configuration operating OGE (AW101 helicopter).

Following sections illustrate the basic elements that compose the SAMA framework, which are the multi-objective genetic algorithm (called GDEA) and the surrogate model (an artificial neural network in the present case). Finally, the SAMA framework itself (called GDMA) is extensively presented.

The Genetic Diversity Evolutionary Algorithm (GDEA)

GDEA [26] is a multi-objective genetic algorithm (MOGA) specifically developed for handling complex aerodynamic optimization problems. The nature of GDEA makes it particularly suitable to incorporate memetic operators as it has two main objectives during a MOOP solution:

1) To drive the search towards the true Pareto-optimal set/front;
2) To prevent premature convergence and distribute the solutions along the set/front itself.

The basic idea of GDEA is to actually use these objectives during the evaluation phase and to rank the solutions with respect to both of them, emphasizing the non-dominated solutions as well as the most genetically different. This results in a selection pressure driving the search simultaneously towards Pareto-optimal and diverse solutions, or, from an equivalent point of view, towards the exploitation of the current non-dominated solutions and the exploration of the search space. GDEA was the GA selected as global searcher for the current optimization problem. The selection of this particular EA was driven by the demand of diversity preservation, especially when the GDEA (or any other GA) is managed by SAMA frameworks. In fact, SAMA strategies tend to increase rapidly the solution convergence resulting, however, in a rapid decrease in genetic diversity.

The Artificial Neural Network as Global Surrogate Model

A generic artificial neural network (ANN) [27] is composed of basic elements, called neurons. Figure 3 shows a general neuron structure: a vector input **p**, with a number Q of elements, is multiplied by the weights w and the solution is added to the bias b. The result is used as an input for the transfer function f, that provides the neuron's output a. The transfer function f can be of different nature, the most commonly used for multi-layer networks are the tan-sigmoid and the linear transfer functions.

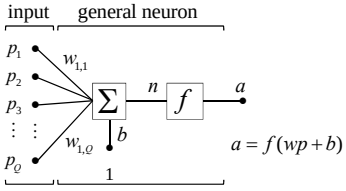

Figure 3: General neuron architecture with input vector.

The neurons are connected together using a structure of links, as in a real biological nervous system. In an ANN the neurons are organized by layers with a finite number of neurons within each layer, and the connections (or weights), together with the biases, can vary their values to modify the response of the network. The ANN always needs a training process to reproduce a generic objective function: during the training, a set of individuals (stored in a database) are considered in relation with their scores. An iterative procedure changes the weights and the biases of the network until a sufficient approximation accuracy of the output data is reached. The original function can be represented following two different strategies:

- **Global Model:** the ANN uses all the available individuals in the database and tries to represent the function for the complete variability range of the parameters. In this case the model is unique and it represents the entire function.
- **Local Model:** the ANN uses just a small part of the available individuals in the database, i.e. the ones closest to the starting individual, so it can represent a limited range of variability of the parameters. In this case the SAMA algorithm needs a new surrogate model for every individual.

In the present work, the first method (Global Model) was used, which is more efficient and requires a single training process for all the individuals.

The particular ANN used here was a feed-forward Back-Propagation Neural Network (BPNN) that was made up of an input, one or more hidden layers, here used with Tan-Sigmoid neurons, and an output layer with a Linear neuron. The Linear neurons were used in the output layer for their non-limited output. Typically, networks with more layers can learn complex relationships more quickly, while layers with more neurons help to fit more complex functions.

Overfitting is one of the most relevant problems in BPNN training: hence, two techniques are usually employed to achieve a good generalization of the solution. The first action to improve generalization is to use a network with a minimum number of neurons, specifically the amount which is just enough to adequate approximation. In fact, larger networks allow fitting more complex problems but they are prone to overfitting the data. The second action is to use the available data to validate the network. The global database, containing input individuals and output solutions from the true objective function, is divided into two subsets. The first one is the training subset, used to train the network. It contains the 75 % of the data, that are chosen randomly. The second one is the evaluation subset, containing the remaining data. The network is trained using the Levenberg-Marquardt algorithm (LM), a quasi-Newton method really faster than the traditional back-propagation. In the present work, the Mean Square Error (*MSE*) was used to measure the BPNN performance, as defined in Eq. (3):

$$MSE = \frac{1}{M_{TDB}} \sum_{i=1}^{M_{TDB}} (F_i - F_{NNi})^2 , \qquad (3)$$

where M_{TDB} is the number of available individuals in the training subset. The iterative training process was stopped when the algorithm reached 100 epochs (iterations), or when the training performance index MSE_{train} was lower than 5×10^{-7}. Finally, the evaluation performance index MSE_{eval} was calculated simulating the trained network with the evaluation subset. The training process was repeated 5 times, since each one has different convergence history, and only the surrogate model with the minimum MSE_{eval} was accepted. The BPNN model used here was developed and adapted from the neural network package of Octave [28].

The Genetic Diversity Memetic Algorithm (GDMA)

GDMA [29] was the algorithm used to perform the optimizations described in the problem formulation section. It is based on a SAMA framework developed from [30] with proper adaptations to the specific global search algorithm (GDEA [26]), local search algorithm (the *fmincon* function within the Matlab® environment [31]) and surrogate model (the BPNN as global metamodel [27]). The course of events during a generic optimization procedure is described in Figure 4 and it can be summarized as follows: the optimization starts with few GDEA generations (the exact number depends on the problem under consideration, on the population size, and other specific considerations): in fact, a minimum number of exact fitness function evaluations are needed to perform a well SM training. Then, the SAMA framework manages the GDEA to create a new population using the typical genetic evolution operators, but all the new individuals are now locally improved before being evaluated by the exact fitness function (the rotor performance solver in the present case). The local improvement is driven by the gradient-based algorithm that, starting from one GDEA's individual, performs its optimization making use of the surrogate and approximated model. A locally improved individual replaces the older one if, and only if, it exhibits an improvement of the objective value. The modified (and hopefully improved) population is finally evaluated using the aerodynamic tool. The process is repeated with another population until the complete convergence or the attainment of the maximum number of exact evaluations. The described technique allows reaching the best compromise between diversity conservation, therefore exploration of new solutions and convergence quickness to the final Pareto front.

The implementation inside the SAMA framework of the gradient-based algorithm for the local improvement leads to several problems connected to the transformation from a general multi-objective problem to a single-objective one, the only supported by the gradient-based algorithm. Different

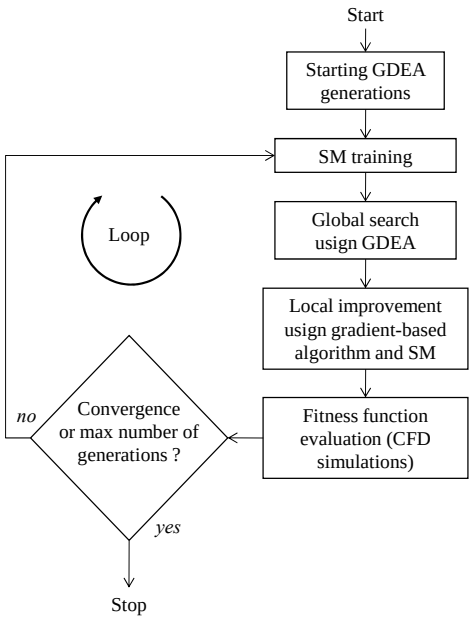

Figure 4: Schematic representation of the GDMA operation.

strategies can be followed to handle this issue. In the present implementation, a multi-objective problem is transformed into a constrained single-objective one. Specifically, the objective to be optimized by the gradient-based algorithm is chosen randomly, while the remaining one is constrained to remain lower than or equal to the starting value.

RESULTS

The innovative optimization strategy (i.e. the GDMA algorithm) developed to improve the efficiency of more common genetic algorithms, has been applied to the problem formulation stated above. CAMRAD/JA solver has been used extensively and the outcomes from this first part of tests is presented. This comprehensive aeromechanical tool is used to validate in a very quick way the entire optimization framework and to demonstrate the effectiveness of blade parameterization based on b-spline curves. The next step carried out was the application of the same methodology to the more accurate (and time consuming) ADPANEL code. Using the latter solver the twist optimization has been repeated highlighting differences and common features respect to CAMRAD/JA. In the final section several comparisons have been performed to show and demonstrate the practical advantages of the GDMA approach respect to a basic genetic algorithm like GDEA, in particular when a computational demanding code is used as flow solver.

Results from GDMA+CAMRAD/JA

The results of the optimizations carried out using CAMRAD/JA are here presented. Three different optimizations of increasing complexity were performed regarding different aspects of the baseline blade configuration. The first one considers a simple twist distribution optimization (Tw), the second one a combined chord-sweep design (Ch+Sw) and the third one all the three features together. Table 4 summarizes the characteristics of these optimization. The three cases have an increasing number of design variables, that can be qualitatively associated to the complexity of the problem. Another important parameter is the population size, a common characteristic of metaheuristic evolutionary algorithms. It represents the number of individuals (in this case an individual is associated to a rotor blade geometry) within a generation. For all optimizations a total number of 40 generations are done, subdivided in 10 initial generations using basic GDEA while the remaining 30 generations with the memetic algorithm GDMA.

Optimization	Features	Design variables	GDMA population
1	Tw	7	40
2	Ch+Sw	13	70
3	Tw+Ch+Sw	20	100

Table 4: Summary of the three optimizations performed using CAMRAD/JA solver.

As previously stated, Table 1 summarizes the flight conditions used for the present optimization. Since the helicopter weight is fixed at 6.5 tons, this problem means nearly to optimize forward flight capabilities of its main rotor at the following two values of disk-loading: $C_T/\sigma = 0.075$ for the condition C1, and $C_T/\sigma = 0.126$ for the condition C2. A multi-objective optimization problem produces as output a set of optimal solutions, defined as Pareto optimal front and made up of all the non-dominated [26] solutions from the entire set of analyzed solutions. Since the problem under consideration is a two-objective problem, a Pareto front is represented by a curve that lies onto a plane. Figure 5 shows the final Pareto fronts from the three different optimizations compared to the baseline rectangular blade rotor. It is possible to note that the first objective Pw_{C1} (that is, the horse power required by the rotor in the condition C1) calculated at sea level experiences much less variation if compared to the second one Pw_{C2} at high altitude (5150 m ASL) that varies from about 1400 up to 2000 Hp. This is certainly due to the higher normalized disk-loading at high altitude that allows, on the contrary, larger improvements during the optimizations, especially in terms of retreating blade stall.

The three Pareto fronts reported in Figure 5 give some useful qualitative information about the best achievable performance of this particular rotor and optimization problem. Optimization 1 and 2 lead to similar performance improvements (note the portion in which the Pareto fronts are almost overlapped) but the twist feature seems to affect performance at sea level as at high altitude (the range of variation is around 100 Hp for both the objectives), while chord and sweep distributions greatly affect the high-altitude condition with minor changes at sea level. This is understandable since no limitations or constraints are set for the solidity of the rotor and even a low increase of it can positively affect the behavior at high altitude, with the drawback of a slight increasing of viscous power at sea level. Optimization 3 entails the complete rotor blade redesign and permits the best performance improvements.

As an example, three solutions of each Pareto front are selected and the corresponding distributions (twist, chord and sweep depending on the particular case) are plotted and compared to the original one. The three solutions are equally distributed along the Pareto front extent to describe the influence of each blade feature.

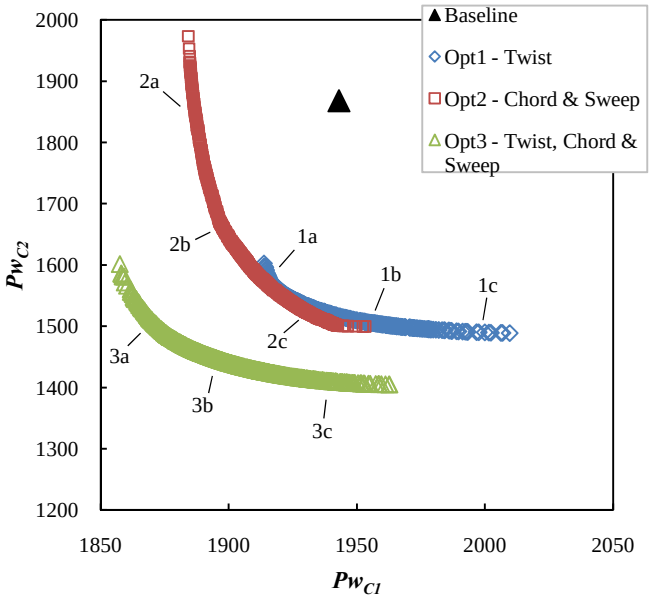

Figure 5: Final Pareto fronts for optimizations performed using CAMRAD/JA, respectively Optimization 1, 2 and 3.

Optimization 1 – Twist

The twist distribution was optimized using CAMRAD/JA and described by means of seven design variables along the entire blade. A total of 1600 individual evaluations were carried out (corresponding to 40 generations with a population size of 40 individuals). Since each objective corresponds to a specific flight condition, double the CAMRAD/JA analyses were performed. The total time required to complete the 40 generations is around 1/2 hour using a quad-core E5607 Intel® Xeon® processor and a single rotor evaluation is carried out in few seconds on a single core. Three solutions from the final Pareto front (visible in Figure 5) are selected (points *1a*, *1b* and *1c*) and compared to the baseline trend in Figure 6. A clear increase in twist slope is observed if compared to the original distribution and all the plotted solutions are highly non-linear. A small central portion remains unchanged for all the optimal solutions but an increasing of the inner twist (from 0.2 to 0.5 r/R) and a slight decreasing of the outer (from 0.8 to 1 r/R) were found to help improving performance at high altitude when comparing the three optimized blades.

Solution called Blade 1b is further analyzed using CAMRAD/JA for three different altitudes (refer to Table 2 for an exact specification) at all the achievable velocities. The horse power levels are plotted in Figure 7 versus the aircraft speed. It can be noted that the sea level condition (Flight1) remains substantially unchanged, while an increasing power reduction can be reached for higher heights. Power is normalized by the density ratio ρ/ρ_0 for clarity. Reduction in power for Blade 1b at C2 optimization condition is around 20%.

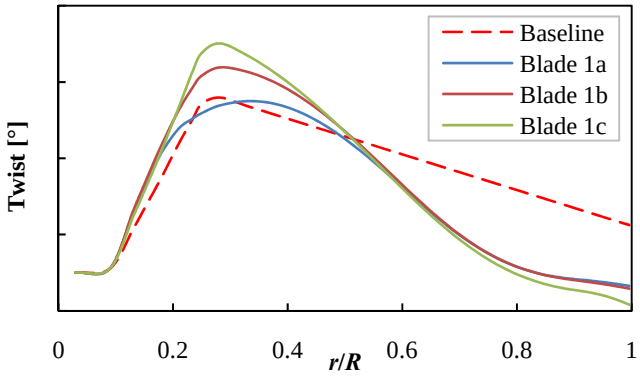

Figure 6: Twist distributions of three Pareto front solutions of the Optimization 1.

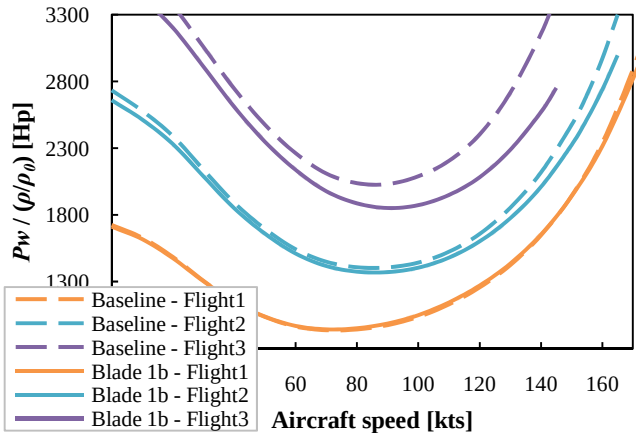

Figure 7: Comparison between Baseline and Blade 1b from Optimization 1. Horse power (normalized by ρ/ρ_0) for different altitudes and velocities.

The same blade is analyzed in terms of local section efficiency (Figure 8) at C2 optimization condition (where the improvements are maximum). Efficiency is enhanced almost everywhere on the disk and particularly on the central portion, with the drawback of a slight reduction in efficiency on the transonic (near the tip) region of the advancing blade, certainly due to more negative local incidences.

Optimization 2 – Chord and Sweep

Optimization 2 redesigns contemporarily chord and sweep of the baseline blade at fixed twist. The population size in this case is 70 and a total of 2800 individuals are evaluated. Also for this optimization three solutions are selected to represent the variation along the final Pareto front (points 2*a*, *2b* and *2c*) and their distributions are visible in Figure 9. The optimum chord trends describe clear physical effects. Firstly, as the power is reduced at higher altitudes the mean chord rises, which means that the rotor solidity rises. It is interesting noting that the chord increasing is gradual but the spanwise location of the maximum chord changes, starting from about 0.7 r/R and going gradually toward inner direction to increase further solidity. The most outer part (above 0.92 r/R) is always equal to the lower admitted bound to reduce transonic effects of the advancing side. The same happens to the inner part (under 0.2 r/R), even if this is due to the typical viscous losses of this region with generation of drag and limited lift. Sweep parameterization is defined from 0.4 r/R up to the blade tip and the final optimal distributions describe typical swept trends. After a recovery of the sweep (from 0.7 to 0.92 r/R) that helps to keep the blade's leading edge fairly straight, the tip zone almost reaches the maximum available sweep. This tip geometry, together with the minimization of chord in this region reduces the compressibility effects, especially in fast forward flight. Blade 2b is analyzed at different altitudes and

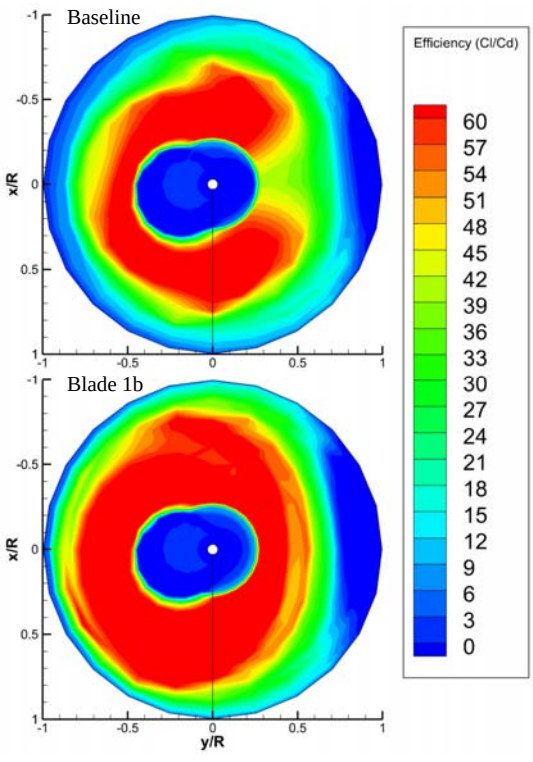

Figure 8: Comparison between Baseline and Blade 1b from Optimization 1. Contour plots of local section efficiency at C2 condition with CAMRAD/JA.

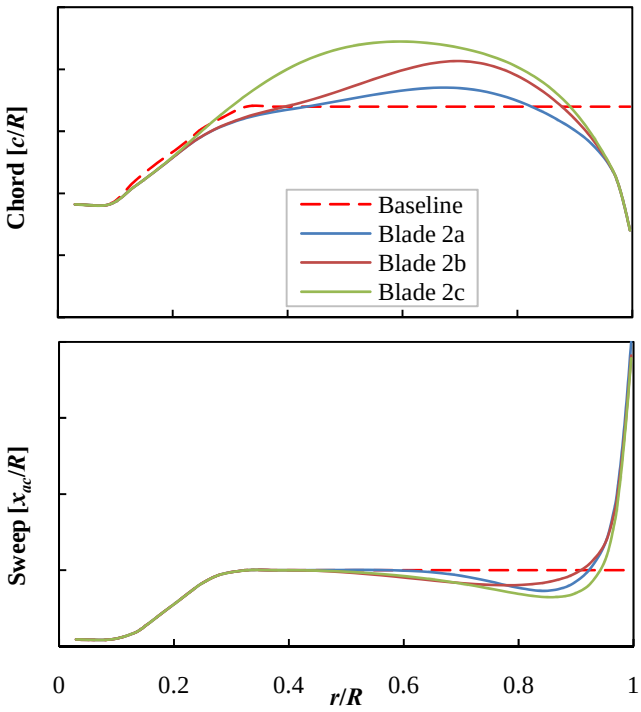

Figure 9: Chord and Sweep distributions of three Pareto front solutions of the Optimization 2.

velocities (Figure 10). The reduction in power at high altitude is lower than the previous Blade 1b where the twist was optimized, but a similar trend is observed in terms of power reduction.

Optimization 3 – Twist, Chord and Sweep

Optimization 3 is the most complex blade design carried out in the present work, due to the high number of design variables (equal to 20 to describe the complete blade). GDMA was run with a population size of 100 individuals for a total number of 40 generations. This means that around 4000 individual evaluations were performed in approximately 2 hours time. Combining the three features (twist, chord and sweep) a remarkable improvement was possible if compared to optimization of lonely twist or chord and sweep (refer to Figure 5 for comparison of the final Pareto fronts). Again three different blades (*3a*, *3b* and *3c*) were selected among the Pareto optimal set and the feature distributions plotted and compared to baseline ones. Comparison between current distributions and the ones from Optimization 1 and 2

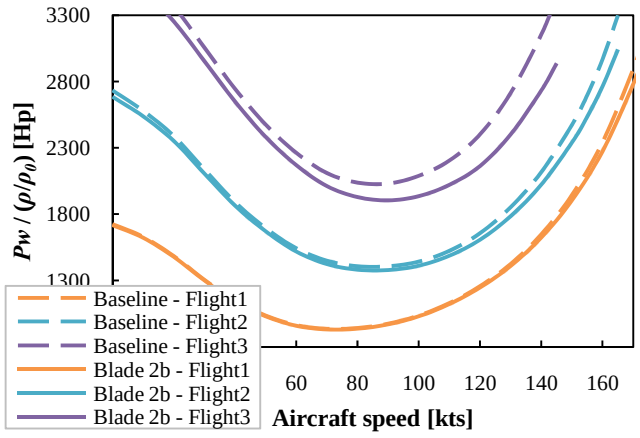

Figure 10: Comparison between Baseline and Blade 2b from Optimization 2. Horse power (normalized by ρ/ρ_0) for different altitudes and velocities.

shows common aspects (Figure 11). Chords describe distributions almost identical respect to Optimization 2 and also sweep is very close to the results of previous case with minor differences: now the tip value reaches the upper admitted bound and the sweep recovery before the tip zone (around 0.8 – 0.9 *r*/*R*) is lower. Twist feature is the most different, although similar behavior is recognized respect to Optimization 1. Reduced twist slopes are clearly visible (certainly due to the contemporarily chord redesign that redistributes local lift) but with identical non-linear trends. The main disparities are localized on twist value at the tip and mostly on the maximum value at inner portion.

The three optimized blades are plotted together in Figure 12 to give also a visual evidence of the tool reliability. It is not uncommon to observe in literature optimization works where remarkable performance results are obtained, which unfortunately lead to unfeasible blades. The present tool seems to be able to optimize rotor blades reaching good performance enhancements and, above all, feasible blade geometries, which is a critical requirement from a manufacturing viewpoint.

Blade 3b is selected for further analyses, visible in Figure 13 and Figure 14. The improvements at high altitude conditions are the maximum observed over the three optimizations. Additional small gains in power are visible also at sea level for high velocities. The comparison of local section efficiency at C2 optimization condition demonstrates

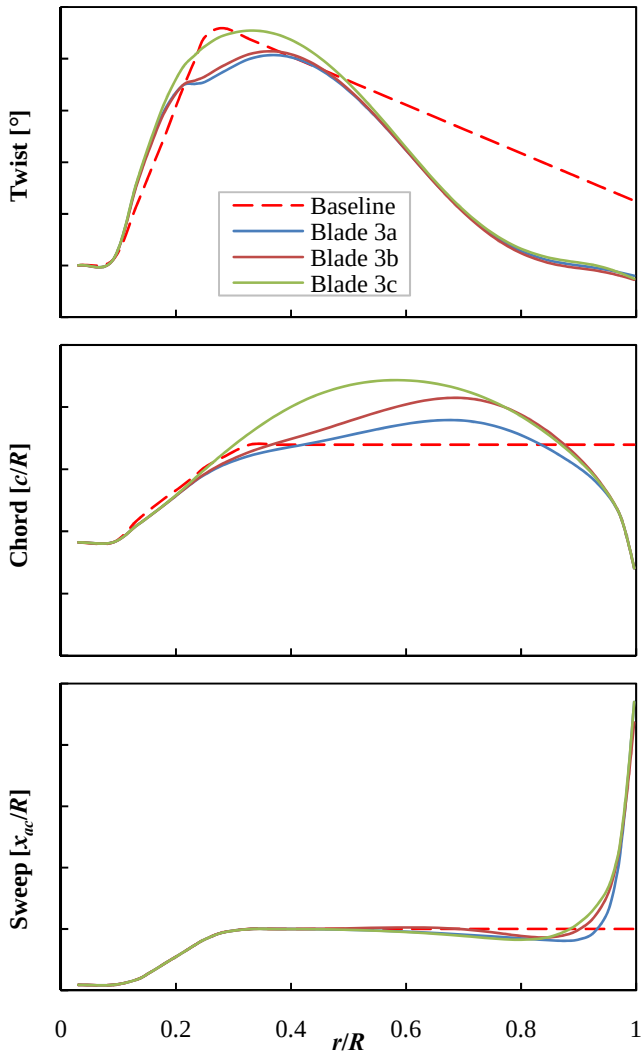

Figure 11: Twist, Chord and Sweep distributions of three Pareto front solutions of the Optimization 3.

Figure 12: Blade plot of three solutions of the Optimization 3, respectively 3a, 3b and 3c blades.

the effects of the blade redesign. Similarly to Optimization 1, even with lower performance of the advancing blade tip region, the remaining part of the disk experiences a large efficiency amelioration.

Results from GDMA+ADPANEL

The three previous optimizations with CAMRAD/JA were carried out to validate the procedure in a quick and rapid manner, while obtaining also remarkable results and a wide survey of the influence of each blade feature on power level in forward flight.

After the validation process, the in-house panel method code ADPANEL has been used to repeat the twist optimization in order to observe differences and similarities with previous results. Outcomes from it are presented in following chapter.

Optimization 4 – Twist

The present optimization problem has the same characteristics of Optimization 1 carried out with CAMRAD/JA solver. The parameterization of the twist distribution is unchanged, having 7 design variables and the same lower/upper bounds. The problem formulation is also unchanged and the optimization conditions remain the two forward flights defined in Table 1. The main difference lies on the flow solver, which is the more accurate ADPANEL code. This new code introduces several complications, related to its nature. First of all, it does not trim automatically the rotor and CAMRAD/JA must be run before to calculate mast inclination, blade flapping motion and cyclic commands. Since the CAMRAD/JA trim does not ensure

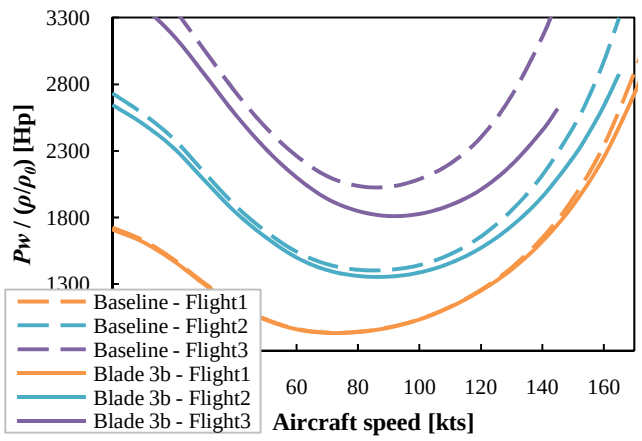

Figure 13: Comparison between baseline blade and 3b blade from Optimization 3. Horse power (normalized by ρ/ρ_0) for different altitudes and velocities.

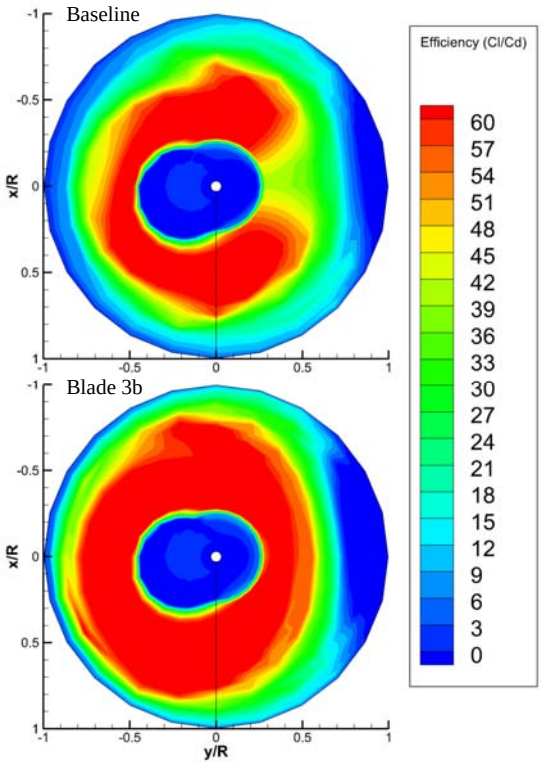

Figure 14: Comparison between Baseline and Blade 3b from Optimization 3. Contour plots of local section efficiency at C2 condition with CAMRAD/JA.

the required thrust level when used in ADPANEL, the rotor collective command is used as an additional design variable and during the optimization the algorithm searches for optimal solutions (in terms of horse power level) but contemporarily trims those solutions. For this reason, the present optimization problem is actually more complex that the one described in Optimization 1, even if the ultimate aim is the same: the twist distribution optimization. In fact, this problem has a total of 9 design variables, 7 describing the twist distribution and 2 collective commands (each one related to a different flight condition); in addition the trim process (in which collective command is calculated to match required thrust) is implemented by means of penalty functions added to each objective of the original objective function (Eq. 1). The second issue arising from ADPANEL is the increased computational demand, which imposes the use of multi-processor computers (cluster) and the consequent remote control from a user terminal, where the real optimization is performed. Analyzing the course of events of Optimization 1 and its convergence history, a more effective strategy was followed, in fact it was observed that 40 generations was an excessive and unnecessary number. The best compromise between rapidity and convergence level was a value between 15 and 20 generations. The latter value was chosen as the current problem is mildly more difficult than Optimization 1 and GDMA algorithm was started just after 4 GDEA's generations (instead of 10, like done in Optimization 1). The population size is unchanged and equal to 40 individuals. This means that about 800 individuals have been evaluated (and 1600 forward flight simulations have been run in ADPANEL). Using 40 processors, the entire process took about 3 days of computation, which means around 6 generations per day.

The final Pareto front is plotted in Figure 15. Since the lower number of generations and higher complexity of the problem, the Pareto optimal set is more scattered than the one

of Optimization 1 and the number of optimal solutions is smaller. Despite this, it is reasonably well converged and all the visible solutions are trimmed to the required thrust force. Again, three solutions were selected and the corresponding twist distributions have been plotted in Figure 16. Twist tends to increase its slope and its maximum value (around 0.28 *r*/*R*) going from solutions 4a to 4c, which corresponds to larger improvement of high-altitude performance. The solutions show highly non-linear trends and, in particular, it seems that ADPANEL was able to capture specific effects that did not arise using CAMRAD/JA. Since the flowfield complexity in case of forward flight and the high variability of section conditions during a single turn, the reason of this particular shape is not completely clear, but it can be associated to three-dimensional effects and/or due to the influence of vortices on the local blade sections.

Solution 4b is selected and the local section efficiency contour plot is compared to baseline blade (Figure 17) for the C2 optimization condition. This optimized blade allows a reduction of power at C2 equal to about 17% maintaining performance at sea level. It is clear that the optimized rotor has improved behavior almost on the entire disk.

For the same blade, a qualitative plot of the free-wake development is plotted in Figure 18 and compared to the baseline blade behavior. From the comparison, it seems that tip vortex of the optimized solution has lower strength (vortices detached from blade tips have lower number of

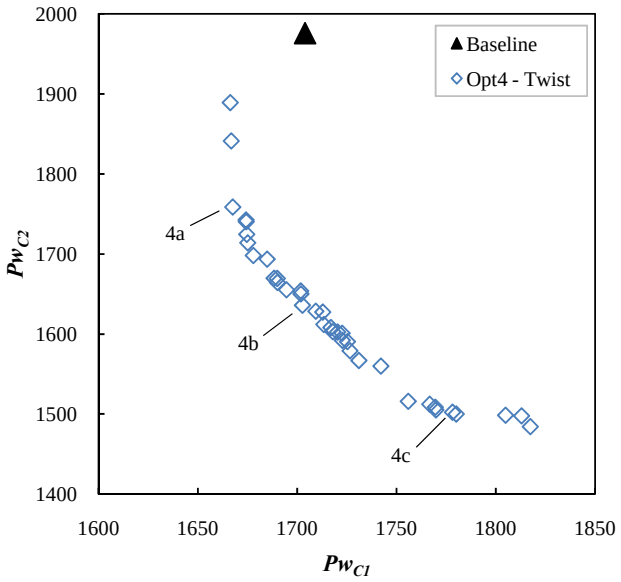

Figure 15: Final Pareto front for Optimization 4 performed using ADPANEL.

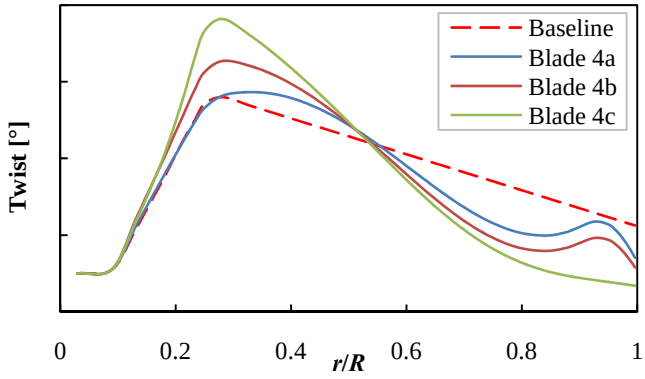

Figure 16: Twist distributions of three Pareto front solutions of the Optimization 4.

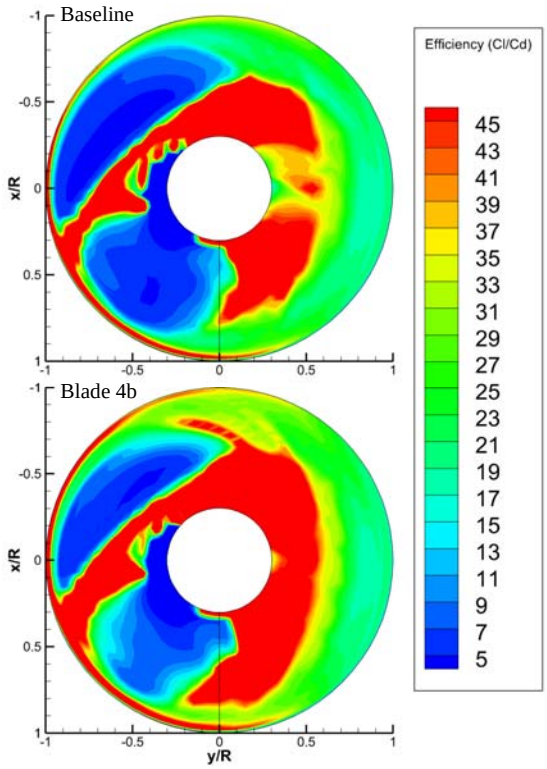

Figure 17: Comparison between Baseline and Blade 4b from Optimization 4. Contour plots of local section efficiency at C2 condition with ADPANEL.

filaments) and in general more distributed and smoother vortex intensity is observed.

Finally, the three twist distributions from the present optimization are compared to the ones found in Optimization 1 using CAMRAD/JA solver (Figure 19). It is worth noting that, a part a small shift of the green dashed curve (Blade 1c), it almost overlaps the Blade 4c twist distribution. Quite similar trends are visible for the other solutions, at least up to 0.5 – 0.6 *r*/*R*. After that the curves have quite different trends, with differences that can reach 2 or 3°. This deviation is due

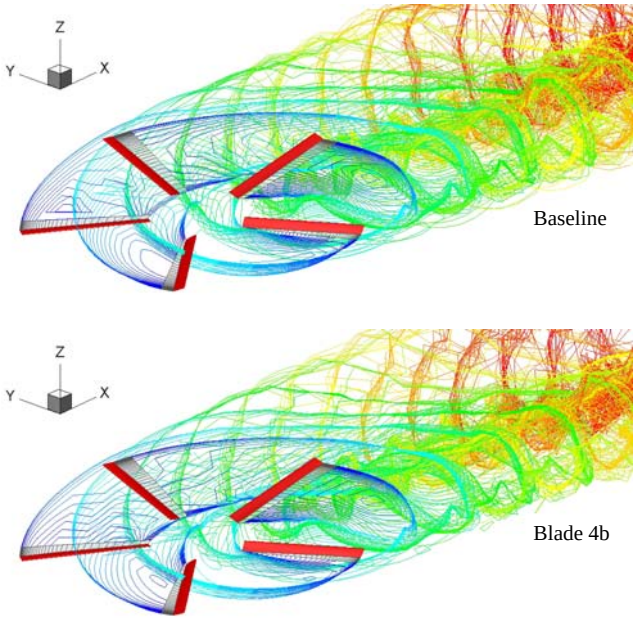

Figure 18: Qualitative comparison of free-wake development between Baseline and Blade 4b from Optimization 4. Calculated at C2 condition with ADPANEL.

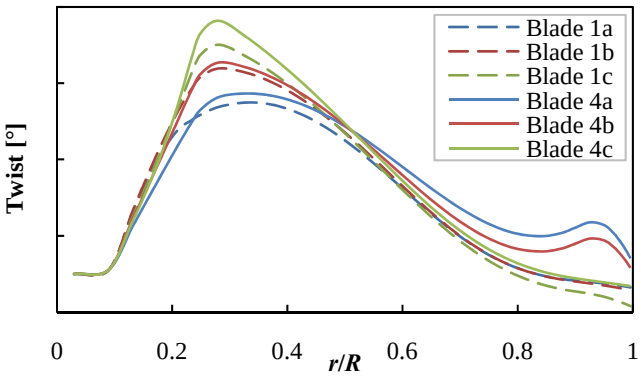

Figure 19: Comparison between twist distributions from Optimization 4 and Optimization 1.

to the aforementioned ability of ADPANEL to capture effects that CAMRAD/JA is not. Nevertheless, we must assert that also CAMRAD/JA seems to be a valid tool for blade development seeing that it was able to catch at least the major features and characteristics of optimized twist distributions.

GDEA-GDMA comparison

A comparison has been carried out to highlight the capabilities of the new optimization framework based on the memetic algorithm GDMA respect to more common optimization techniques like, for instance, basic multi-objective genetic algorithms, available within the framework itself (i.e. GDEA). To do this the most complicated optimization problem has been selected among the previous ones, which is the Optimization 3 test, where all the blade features were optimized contemporarily (twist, chord and sweep) and a total of 20 design variables were present. Additional tests (not reported here for brevity) demonstrated that GDMA's advantages arise in particular when the number of design variables (proportional to problem complexity) is higher than about 8-10. For lower values GDMA is anyway superior but differences are smaller and GDEA is able to get an almost complete convergence in a reasonable amount of aerodynamic simulations. The performances of the two algorithms were evaluated with the same problem and settings. The basic genetic algorithm, GDEA, was run for 40 generations and a total number of 4000 individual evaluations. GDMA was started after 10 initial GDEA's generations and 30 additional generations were performed by means of the memetic framework. In this manner, the same individuals (aerodynamic simulations) were evaluated, requiring approximately the same time. This means that after the first 10 generations the results in terms of Pareto optimal front are identical for both the algorithms. For this reason in Figure 20 the Pareto fronts of the competing algorithms are plotted at several generations starting from 12 (just above GDMA's activation) increasing up to 40. The superiority of GDMA approach is clear already after 2 generations from its activation and is almost constant in all the six plots shown. After 15 generations the GDMA's Pareto front is stabilized and further calculations just contribute to intensify density and enlarge Pareto spread.

This example evidences the advantages of GDMA and its abilities to deal with highly complex optimization problems. First of all, this approach helps to reach a wide convergence level that is not possible with other traditional algorithms (to be run within reasonable computational time), which means, in this case, more improved optimal blades. Secondly, the final Pareto optimal front has improved density and a larger set of optimal solutions. This aspect is not marginal since it allows the designer to choose from a wider range of options. Finally, the most important benefit is certainly the higher efficiency (also defined as convergence rate) which permits to reduce the total number of function evaluations to obtain the same solution improvement. In fact, observing again Figure 20, we can state that carrying out just 15 generations with GDMA we obtained the same or better solutions than after 40 generations of the basic GDEA. This result was already used in Optimization 4 (performed with ADPANEL) to reduce to minimum the number of simulations and the corresponding computational time, and it could be a central aspect in case of even more computational demanding codes, like Navier-Stokes solvers.

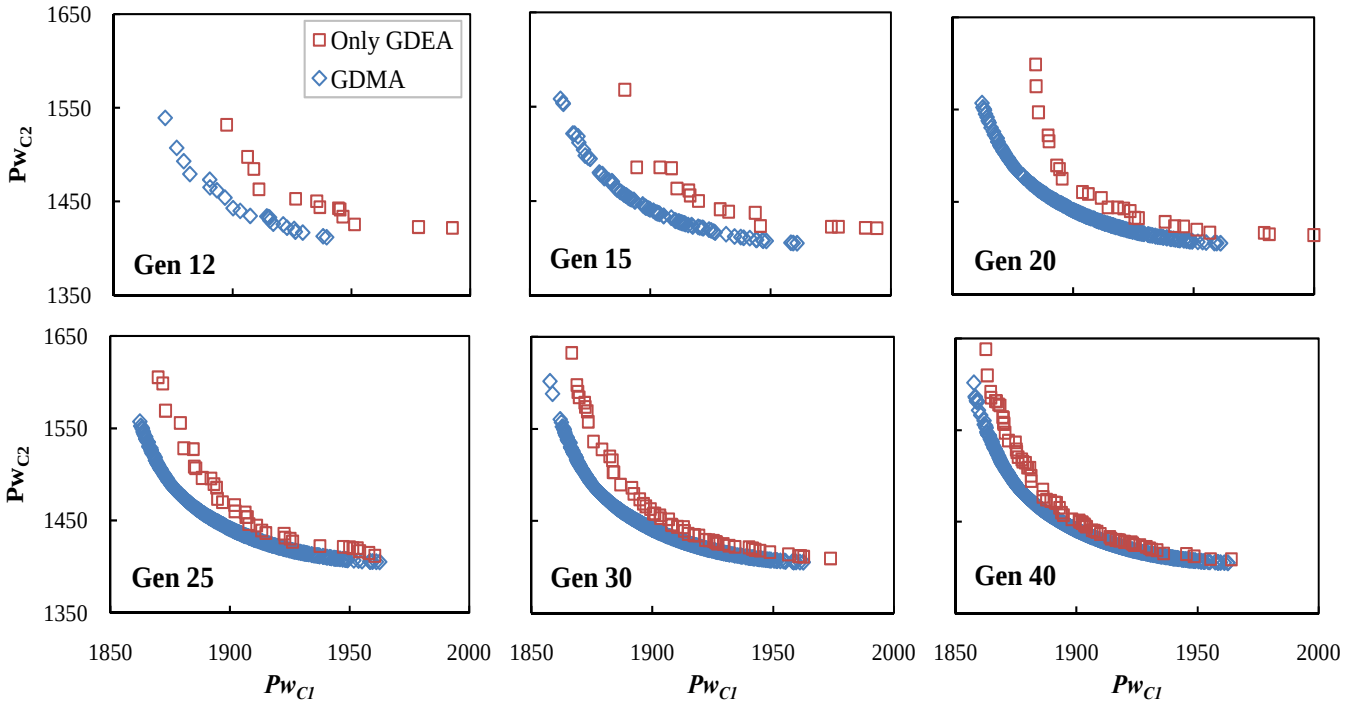

Figure 20: Comparison between GDMA and the basic GDEA performance. Test carried out over the Optimization 3 problem.

CONCLUSIONS

An optimization framework for helicopter rotor blade design has been developed, which is based on state-of-the-art multi-objective surrogate-assisted memetic algorithm coupled with different aerodynamic tools, like CAMRAD/JA and in-house developed ADPANEL solver, a three-dimensional panel method with CVC free-wake vortex model. This optimization methodology has been applied to the redesign of a main rotor with rectangular blades in forward flight as an example. Several blade features were considered during the tests, like twist, chord and sweep, first separately and then together.

Comparison of final Pareto optimal fronts and optimized blade solutions yield the following specific conclusions:

- GDMA optimization strategy demonstrated to be a valid and efficient tool for rotor blade optimizations. The advantage of a real multi-objective (and multi-point) approach is present, while the main drawback of genetic algorithms, which is the large number of evaluations, is mitigated by the use of surrogate models and local search with gradient-based algorithms. Multi-objective approach is used here to deal with different forward flight conditions, but it can be extended (with limited additional computational efforts) to more challenging problems like hover-forward flight blade shape optimizations.
- GDMA showed also to be superior to more traditional optimization methods like genetic algorithms, obtaining more improved optimal solutions with minimum value of aerodynamic rotor simulations. This is an essential characteristic to make possible in the close future the coupling of this multi-objective optimization strategy with highly complex and computational demanding aerodynamic tools, like Navier-Stokes solvers.
- Both CAMRAD/JA and ADPANEL codes proved to be flexible and capable tools for coupling with fully automated optimization frameworks. Furthermore, from a manufacturing viewpoint, feasible blade geometries were obtained for all the tests performed. It is worth noting that this important result is also due to excellent capabilities of b-spline curves as blade shape parameterization.
- Remarkable results were obtained in terms of horse power reduction, particularly at high altitude operations. In this conditions, since the high normalized disk-loading, large improvement margin is possible and a reduction between 12% and 24% respect to the baseline blade was obtained from numerical computations. This ameliorations lead not only to power decrease but also to a possible extension of maximum aircraft speed. Limited variations are encountered at sea level, on the order of 50-100 Hp.
- Many information were obtained from the final optimized solutions. Optimal twist distributions showed to be highly non-linear with greater twist slope around the central blade portion respect to the baseline and a gradual reduction of the slope itself from 0.8 r/R up to the tip. Swept blades were found when chord and sweep features were taken into account. Chord trends reached lower bound around tip zone to better uniform lift distribution and reduce tip vortex influence. Maximum chord value is located around blade center and tends to increase as power at high height goes down, accordingly to the typical effect of solidity growth. Sweep starts from about 0.9 r/R and tends to reach the maximum available value, to minimize compressibility effects.
- Similar twist distributions were found comparing results from CAMRAD/JA and ADPANEL, proving that the basic features of the flowfield over the rotor were captured also by the simpler lifting-line solver, like slope and general trend. Nevertheless, ADPANEL seems to be able to gather more detailed information of blade loading and three-dimensional effects, as demonstrated by the quite different shape of tip blade twist obtained by means of the panel method.

REFERENCES

[1] Celi, R., *"Recent Applications of Design Optimization to Rotorcraft – A Survey"*, Proceedings of the 55th Annual Forum of the American Helicopter Society. Montréal, Canada. May 25-27, 1999.

[2] Ganguli, R., *"Survey of Recent Developments in Rotorcraft Design Optimization"*, Journal of Aircraft, Vol. 41, No. 3, 2004, pp. 493-510.

[3] Myers, R. H., Montgomery, D. C., Anderson-Cook, C. M., *"Response Surface Methodology: Process and Product Optimization Using Designed Experiments"*, 3rd edition, John Wiley & Sons, 2009.

[4] Walsh, J. L., *"Performance Optimization of Helicopter Rotor Blades"*, NASA-TM-104054, 1991.

[5] Johnson, W., "*Camrad/JA - A Comprehensive Analytical Model of Rotorcraft Aerodynamics and Dynamics - Volume II: User's Manual*", Johnson Aeronautics, 1988.

[6] Vanderplaats, G. N., *"CONMIN - A Fortran Program for Constrained Function Minimization"*, User's Guide, NASA-TM-X-62282, 1973.

[7] Walsh, J. L., LaMarsh, W. J., Adelman, H. M., *"Fully Integrated Aerodynamic/Dynamic Optimization of Helicopter Rotor Blades"*, NASA-TM-104226, 1992.

[8] Straub, F. K., Callahan, C.B. and Culp, J. D., *"Rotor design optimization using a multidisciplinary approach"*, Structural Optimization, Vol. 5, 1992, pp. 70-75.

[9] Rand, O., Khromov, V., Peyran, R. J., *"Minimum-Induced Power Loss of a Helicopter Rotor via Circulation Optimization"*, Journal of Aircraft, Vol. 41, No. 1, 2004, pp. 104-109.

[10] Walsh, J. L., Young, K. C., Pritchard, J. I., Adelman, H. M., and Mantay, W. R., *"Integrated Aerodynamic/Dynamic/Structural Optimization of Helicopter Rotor Blades Using Multilevel Decomposition"*, NASA-TP-3465, 2005.

[11] Henderson, J. L., Walsh, J. L., and Young, K. C., *"Application of Response Surface Techniques to Helicopter Rotor Blade Optimization Procedure"*, NASA-TM-111274, 2005.

[12] Le Pape, A., Beaumier, P., *"Numerical Optimization of Helicopter Rotor Aerodynamic Performance in Hover"*, Aerospace Science and Technology, Vol. 9, 2005, pp. 191-201.

[13] Soto, O., Lohner, R., and Yang., C., *"An Adjoint-Based Design Methodology for CFD Problems"*, International Journal of Numerical Methods for Heat and Fluid Flow, Vol. 14, 2004, pp. 734–759.

[14] Lee, S. W., and Kwon, O. J., *"Aerodynamic Shape Optimization of Hovering Rotor Blades in Transonic*

Flow Using Unstructured Meshes", Journal of Aircraft, Vol. 44, No. 8, 2006, pp. 104-109.

[15] Dumont, A., Le Pape, A., Peter, J., Huberson, S., *"Aerodynamic Shape Optimization of Hovering Rotors Using a Discrete Adjoint of the RANS Equations"*, Proceedings of the 65th Annual Forum of the American Helicopter Society, Grapevine, Texas, May 27-29, 2009.

[16] Nielsen, E. J., Lee-Rausch, E. M., Jones, W. T., *"Adjoint-Based Design of Rotors Using the Navier-Stokes Equations in a Noninertial Reference Frame"*, Proceedings of the 65th Annual Forum of the American Helicopter Society, Grapevine, Texas, May 27-29, 2009.

[17] Anh Vu, N., Lee, J. W., Byun, Y. H., Kim, S., *"Aerodynamic Design Optimization of Helicopter Rotor Blades including Airfoil Shape"*, Proceedings of the 66th Annual Forum of the American Helicopter Society, Pheonix, Arizona, May 11-13, 2010.

[18] Johnson, C. S., Barakos, G. N., *"Optimizing Aspects of Rotor Blades in Forward Flight"*, 49th AIAA Aerospace Sciences Meeting including the New Horizons Forum and Aerospace Exposition, Orlando, Florida, 4-7 Jan. 2011.

[19] D'Andrea, A., *"Development of a Multi-Processor Unstructured Panel Code Coupled with a CVC Free Wake Model for Advanced Analyses of Rotorcrafts and Tiltrotors"*, Proceedings of the 64th Annual Forum of the American Helicopter Society, Montréal, Canada, Apr. 29-May 1, 2008.

[20] Rogers, D. F., *"An Introduction to NURBS With Historical Perspective"*, Elsevier, 2001.

[21] Verna, A., D'Andrea, A., *"Unsteady Simulations of Rotorcraft in Ground Effect using a Fast Panel-Fast Vortex Formulation"*, Proceedings of the 35th European Rotorcraft Forum, Hamburg, Germany, Sep. 22-25, 2009.

[22] D'Andrea, A., *"Numerical Analysis of Unsteady Vortical Flows Generated by a Rotorcraft Operating on Ground: a First Assessment of Helicopter Brownout"*, Proceedings of the 65th Annual Forum of the American Helicopter Society, Grapevine, Texas, May 27-29, 2009.

[23] D'Andrea, A., Scandroglio, A., Melone, S., *"Numerical Analysis of Advanced-Innovative Tiltrotor Configurations"*, Proceedings of the 34th European Rotorcraft Forum, Liverpool, UK, Sep. 16-19, 2008.

[24] Lim, D., Jin, Y., Ong, Y. S., Sendhoff, B., *"Generalizing Surrogate-Assisted Evolutionary Computation"*, IEEE Transactions on Evolutionary Computation, Vol. 14, No. 3, 2010, pp. 329-355.

[25] Ong, Y.-S., Krasnogor, N., Ishibuchi, H., *"IEEE Transactions on Systems, Man and Cybernetics - Part B: Special Issue on Memetic Algorithms"*, Vol. 37, Issue 1, 2007, pp. 2-5.

[26] Toffolo, A., Benini, E., *"Genetic Diversity as an Objective in Multi-Objective Evolutionary Algorithms"*, Evolutionary Computation, Vol. 11, Issue 2, 2003, pp. 151-167.

[27] Hagan, M. T., Demuth, H. B., Beale, M., *"Neural Network Design"*, PWS Publishing Company, 1996.

[28] Schmid, M. D., *"A neural network package for Octave - User's Guide - Version: 0.1.9.1"*, 2009.

[29] Massaro, A., Benini, E., *"A Surrogate-Assisted Evolutionary Algorithm Based on the Genetic Diversity Objective"*, submitted to IEEE Transactions on Evolutionary Computation, Mar. 2011.

[30] Lim, D., Jin, Y., Ong, Y. S., Sendhoff, B., *"A Study on Metamodeling Techniques, Ensembles, and Multi-Surrogates in Evolutionary Computation"*, GECCO'07, Jul. 7-11, 2007, pp. 1288-1295.

[31] The Mathworks, *"Matlab R2009a Guide"*, 2009.